

## Point-to-point response

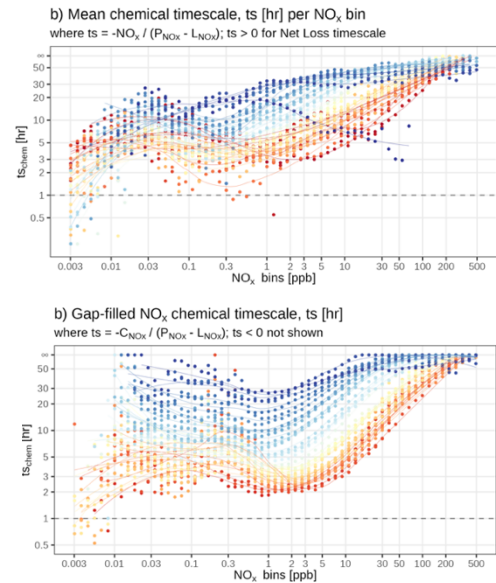
We thank two reviewers for their constructive comments and have addressed all comments with additional analyses and clarifications to the manuscript. We start the response with a summary of changes for both reviewers. Our point-to-point responses are highlighted in blue with track changes in blue/red and reviewers' comments in black.

## General responses to both reviewers

Two main criticisms from the two reviewers include:

- 1) Omission of chemical pathways and processes (heterogeneous NO<sub>x</sub> chemistry, NO + HO<sub>2</sub>/RO<sub>2</sub>);
- 2) Lagrangian atmospheric mixing (mixing scales in PBL, mixing between FT and ML).

We also identified a minor bug in the estimated NO<sub>x</sub> net timescales and reran simulations. The main difference from the initial submission (**upper right panel**) is the timescale over NO<sub>x</sub>-limited regimes at high SZA bins (NO<sub>x</sub> < 0.1 ppb and SZA > 50 degrees in the **lower right panel**).



As changes in the TROPOMI version and model parameters may affect model-data comparisons, we summarize the model-data slopes for all overpasses over the New Madrid power plant based on each configuration (**Fig. R1 below**). All simulations presented here used EPA emissions and 3km HRRR meteorological fields. Similar to **Fig. 6**, not accounting for NO<sub>x</sub> chemistry results in a positive model bias of tNO<sub>2</sub> (**blue crosses in Fig. R1**); and using the latest TROPOMI version (v2.3 from v1.3) has largely reduced the model-data mismatches (**orange circles to orange dots**). The minor correction in the derived net loss timescale and the mixing time scale (from 3 to 1hr) only slightly alter the model-data slopes (**orange dots vs. purple dots vs. purple crosses**).

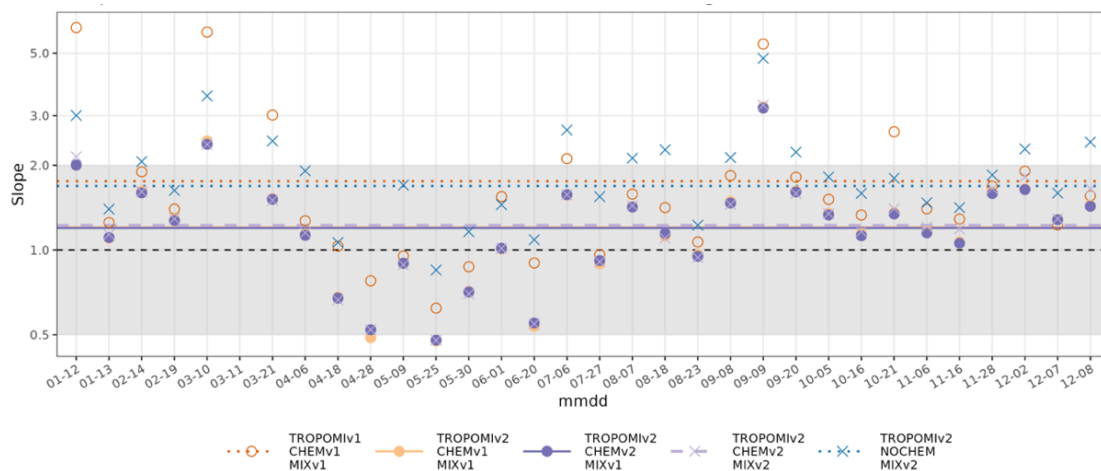


**Figure R1.** Model-data comparisons informed by the linear slope between the two using different versions (v1/v2) are explained as follows: **TROPOMI**: v1.3 or v2.3 of the TROPOMI L2 NO<sub>2</sub> retrieval. **CHEM**: v1 vs. v2 for runs using NO<sub>x</sub> curves from the initial vs. revised manuscript (as shown in the above comparison). **MIX**: inter-parcel mixing with two different horizontal mixing timescales tested (3 vs. 1 hr) over a 1km box. Tests with a spectrum of mixing parameters have been conducted in response to the 1<sup>st</sup> comment of reviewer 2.

### Comments from reviewer #1

Satellite retrievals of NO<sub>2</sub> columns are used to determine NO<sub>x</sub> emissions from power plants and cities. They are increasingly used alongside CO<sub>2</sub> retrievals to calculate emissions from these sources. However, the effect of NO<sub>x</sub> chemistry and transport on NO<sub>2</sub> columns is often overlooked. To address this issue, Wu et al. have developed a model that incorporates a simplified representation of NO<sub>x</sub> chemical loss within the STILT Lagrangian particle dispersion model. It includes additional features such as a column weighting module to account for retrieval averaging kernel profiles and an error analysis module. The model is evaluated against TROPOMI NO<sub>2</sub> observations from three power plants and two cities. The manuscript covers the model's advantages, limitations, and applications such as using NO<sub>2</sub>-to-CO<sub>2</sub> enhancement ratios to estimate CO<sub>2</sub> emissions and identifying wind biases in meteorological data.

While this work is generally sound and well-presented, there are areas that I think need attention.

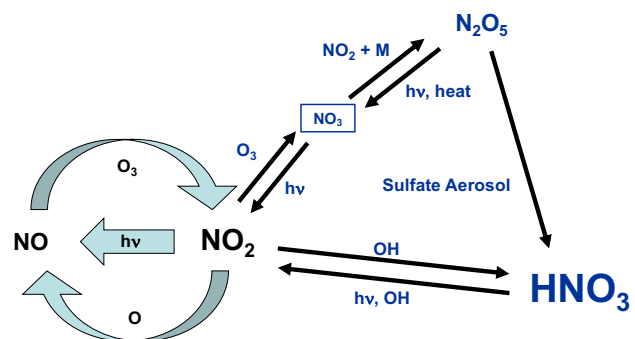
We appreciate the constructive comments from Reviewer #1 and tried to address all concerns via additional supporting analyses.

NO<sub>x</sub> chemical tendency (Sect. 2.1):

1. It appears that the model excludes heterogeneous NO<sub>x</sub> chemistry in aerosols. If this is indeed the case, it is important to discuss the resulting errors arising from this omission.

Alternatively, if heterogeneous NO<sub>x</sub> chemistry is included, please clarify, and modify Fig. 1 accordingly to reflect this information.

The gas-aerosol chemistry of NO<sub>x</sub> was not turned on in WRF-Chem as properly addressing such reactions requires knowledge about aerosol loading and composition as well as uncertainties in the dependence of reaction probability on water vapor and temperature (e.g., Real et al., 2008), which remain challenging topics. Certainly, the N<sub>2</sub>O<sub>5</sub> hydrolysis is an important NO<sub>x</sub> pathway during nighttime. Essentially, we did not enable the arrow from N<sub>2</sub>O<sub>5</sub> to HNO<sub>3</sub> given our choice of WRF-Chem (see simplified diagram above). Note that RACM considers the thermal decomposition of N<sub>2</sub>O<sub>5</sub> (Stockwell et al., 1997).

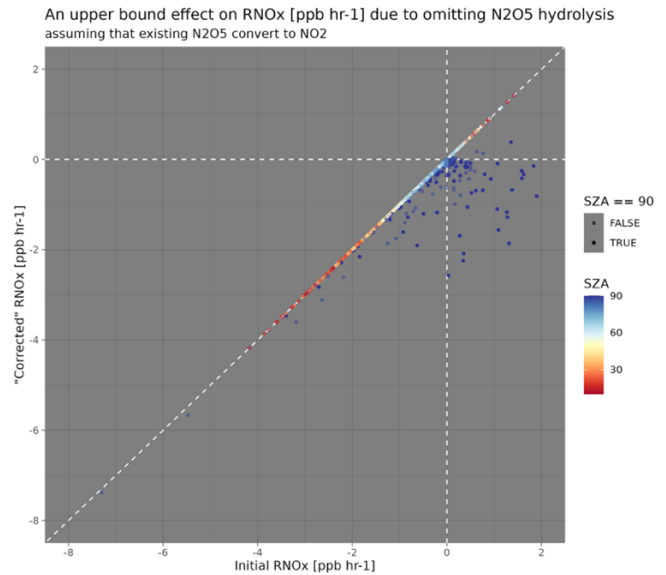


As a result, more NO<sub>x</sub> will survive the night and appear in the morning due to the photolysis and thermal decomposition of N<sub>2</sub>O<sub>5</sub> instead of being partially lost to HNO<sub>3</sub>. The omission of N<sub>2</sub>O<sub>5</sub> hydrolysis generally causes a high bias in NO<sub>2</sub> concentration and a resulting slow bias in the chemical loss of NO<sub>x</sub> over urban environments. In other words, the NO<sub>x</sub> chemical tendency (RNO<sub>x</sub> = PNO<sub>x</sub> - LNO<sub>x</sub>) is larger in the atmosphere (i.e., faster NO<sub>x</sub> loss rate) than in the model.

To address this comment, we added a simple sensitivity experiment to understand the impact of the omission of N<sub>2</sub>O<sub>5</sub> hydrolysis via simple sensitivity analysis. For this experiment, we simply

assume that all existing N2O5 in the current setup of WRF-chem photolyzed into NO<sub>2</sub> during the day (SZA < 90), despite those N2O5 being extracted from the non-hydrolysis runs. We then update the bin-averaged NO<sub>x</sub> chemical tendency and compare it with the original. Reduction in chemical tendency is found for each 2-deg SZA bin and a maximum reduction occurs at SZA of ~90 degrees (**blue dots in the figure to the right**).

Nonetheless, considering the local overpass time of TROPOMI of ~1 pm, we expect the impact to become progressively small as the plume disperses. In other words, it becomes more of a background issue/bias, which may not greatly affect the future emission estimates if the background is properly subtracted from both TROPOMI and the model.



2. The NO<sub>x</sub> chemical tendency is parameterized as a function of NO<sub>x</sub> concentration and the solar zenith angle. It is unclear why these were the only two variables chosen and whether they account for most of the variation in the NO<sub>x</sub> chemical tendency. Knowing the fraction of variation explained by these variables would be useful. I expected temperature (as a proxy for seasons) and the NO<sub>2</sub>/NO ratio to be potentially important variables.

We agree that we did not explicitly show to what degree the variability in NO<sub>x</sub> chemical tendency is explained by the chosen two variables. Although adding feature variables to the NO<sub>x</sub> curves will necessarily explain more variability of NO<sub>x</sub> chemical tendencies (RNO<sub>x</sub>) when training RNO<sub>x</sub>, some feature variables are difficult to “obtain” or only have a marginal effect in predicting RNO<sub>x</sub>. Our rationale is to choose environmental variables compared to atmospheric concentrations of other tracers like ozone unless possible “proxies” are available for those tracers’ abundance.

To justify our choices and inform the “fraction of variation explained by these variables” as suggested by the reviewer, we conducted sensitivity analyses. The grid-level RNO<sub>x</sub> is grouped and averaged into bins of feature variables so that the variability in initial RNO<sub>x</sub> will be damped after grouping. Here we compared the initial RNO<sub>x</sub> derived from WRF-chem and the bin-averaged RNO<sub>x</sub> and reported their Pearson correlation coefficient and RMSE (**see figure shown below, now as Fig. S2a and S2b in the revised manuscript**). Those two statistical metrics were reported for every choice of variables and four scenarios with higher vs. lower NO<sub>x</sub> levels (orange vs. blue bars) and day vs. nighttime (empty bars vs. bars with stripes).

The variability in RNO<sub>x</sub> is better preserved as more variables are considered especially when NO<sub>x</sub> is high, i.e.,  $\geq 1$  ppb (**orange bars in Fig. S2a**). Although the correlation remains low for lower NO<sub>x</sub> conditions ( $< 1$  ppb), the chemical tendencies stay low, leading to small absolute random errors (**Fig. S2b**). Nonetheless, including NO<sub>2</sub>/NO ratio and VOCR seems to have marginal impacts

on preserving RNO<sub>x</sub> variability over polluted regions. Introducing ozone concentration would help, but the prediction of ozone is arguably more complicated than the prediction of NO<sub>x</sub>. The correlation coefficient improves when adding air temperature, but RMSE does not largely reduce.

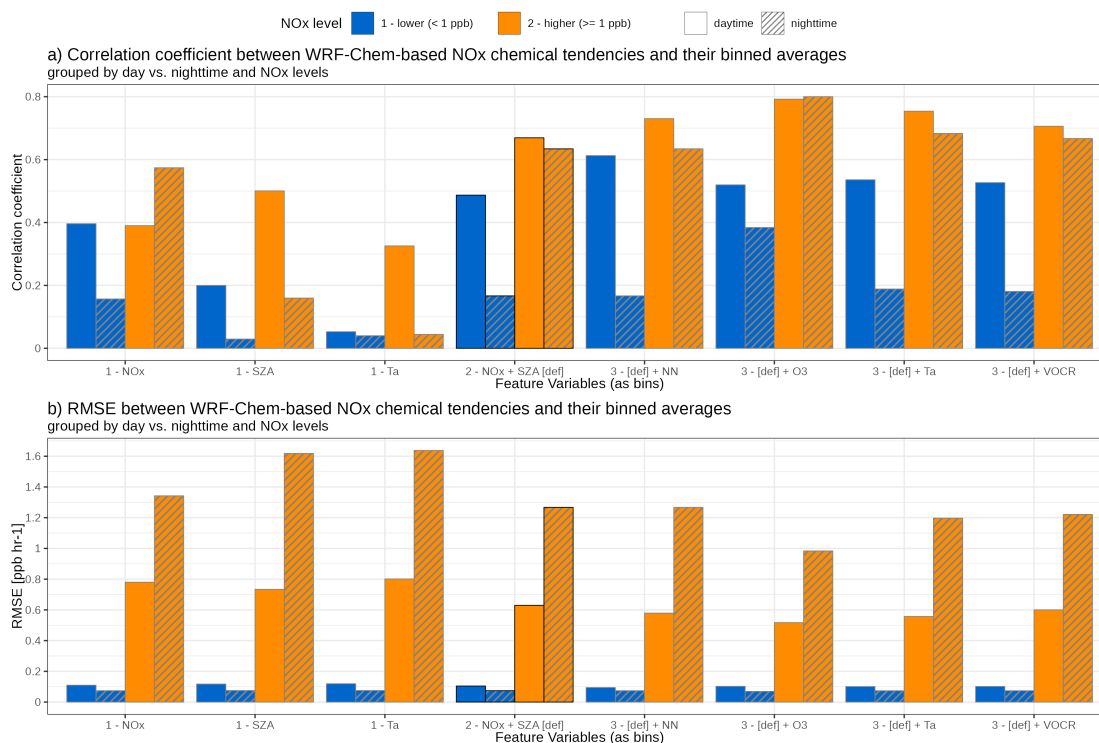


**Figure S2 (ab)** Correlation coefficient and RMSE between the raw RNO<sub>x</sub> directly derived from WRF-Chem and the bin-averaged RNO<sub>x</sub> based on 8 combinations of feature variables. The number in front of the feature variables on the x-axis denotes the total # of variables used when grouping the raw RNO<sub>x</sub>. The combination we used (2-NO<sub>x</sub>+SZA for NO<sub>x</sub> concentration and solar zenith angle, SZA) is highlighted in bars with black outlines. Additional variables tested include air temperature (Ta), NO<sub>2</sub>-to-NO<sub>x</sub> ratio (NN), ozone (O<sub>3</sub>), and VOC reactivity (VO<sub>CR</sub>). Results are reported separately for higher or lower NO<sub>x</sub> levels (orange or blue) during the day or night (empty bars or bars with strips).

In conclusion, we chose two variables in this version: 1) NO<sub>x</sub> concentration for initiating its non-linear dependence on chemical tendency, and 2) SZA for indicating photolysis rates. We have acknowledged that these NO<sub>x</sub> curves/relationships can be improved and replaced using more variables or different chemical schemes. In particular, the addition of background ozone if properly constrained would be an important advance (which also helps constrain the NO<sub>2</sub>-to-NO<sub>x</sub> ratio). **We now added a brief explanation in Sect. 2.1:**

215 The above grouping procedure of  $R_{NO_x}$  based on a finite number of bins of  $C_{NO_x}$  and  $\theta$  unavoidably reduces the variability of  $R_{NO_x}$  that were directly derived from WRF-Chem. To assess the extent to which the  $R_{NO_x}$  variability can be explained by the selected binning feature variables, we performed a sensitivity test to quantify the deviation of bin-averaged  $R_{NO_x}$  from the initial  $R_{NO_x}$ . Generally, the  $R_{NO_x}$  variability is better preserved over polluted regimes with higher NO<sub>x</sub> level > 1 ppb than over low-NO<sub>x</sub> regimes (Supplement Figs. S2ab). Choosing  $C_{NO_x}$  alone better explains the  $R_{NO_x}$  variability than choosing SZA or air temperature alone. Including additional variables (e.g., air temperature, NO<sub>2</sub>-to-NO<sub>x</sub> ratio, and VO<sub>CR</sub>) on top of our default choice of SZA and  $C_{NO_x}$  marginally improves the prediction of  $R_{NO_x}$  except for the inclusion of ozone. However, estimating ozone remains a challenging problem, thereby ozone is not included as a feature variable in this study.

3. The calculation of the NO<sub>x</sub> chemical tendency was based on WRF-Chem simulations for three cities: Los Angeles, Shanghai, and Madrid. The rationale behind selecting these specific cities seems arbitrary. They are unrelated to the power plants and cities that were chosen for model evaluation. It would be helpful to have an explanation for this choice.

LA, Shanghai, and Madrid represent typical megacities in North America, Asia, and Europe and are chosen given their distinct sectoral emissions of GHGs, NO<sub>x</sub>, and VOCs. The fact that the three training cities don't overlap with the targets for predictions is in turn a benefit, which avoids possible overfitting of the NO<sub>x</sub> tendency relationships with feature variables. If we trained and then tested over the same three cities, it would be less convincing in terms of the generalization of the model parameterizations. **We add a brief explanation In Sect. 2.1:**

180 ~~Considering urban areas being the main focus of our study~~Focusing primarily on polluted environments, we carried out WRF-Chem simulations ~~over for~~ for three mid-latitude cities and ~~focused on outputs over extracted model outputs from~~ a 2° × 2° region around the city center to spotlight chemical regimes in urban environments. The three cities are centered around each city. Three cities, namely Los Angeles in the US, Shanghai in China, and Madrid in Spain  ~~, which varied in and VOC emissions and climatology.~~ represent typical megacities in North America, Asia, and Europe. Their varied climatic conditions and sectoral emissions of NO<sub>x</sub>, VOC, and GHGs provide a holistic view of the variability of NO<sub>x</sub> chemical tendency. While our analyses  
185 extended to power plants and cities beyond these three training sites when compared to TROPOMI data (Sect. 4), it helps assess the broader applicability of our chemical parameterizations.

4. The assumption of the NO<sub>x</sub> chemical tendency being independent of height (Eq. 2) is not accurate considering the vertical gradients of NO<sub>x</sub> near the surface during nighttime and early mornings. It seems important to discuss any limitations arising from this.

We apologize for the misleading text and Eq. 2 and clarify that NO<sub>x</sub> chemical tendency (RNO<sub>x</sub>) is not assumed to be independent of height. Since RNO<sub>x</sub> relies on NO<sub>x</sub> concentration (CNO<sub>x</sub>) and CNO<sub>x</sub> varies vertically, RNO<sub>x</sub> varies with altitude. We clarify that both RNO<sub>x</sub> and CNO<sub>x</sub> were extracted from each WRF-Chem model grid and from 12 levels within the boundary layer. Those RNO<sub>x</sub> and CNO<sub>x</sub> were further grouped up to create those NO<sub>x</sub> curves in **Figure 3**. When it came to predicting CNO<sub>x</sub> in STILT-NO<sub>x</sub>, modeled NO<sub>x</sub> concentrations vary between STILT air parcels at different vertical levels because STILT footprint takes care of the atmospheric transport, and RNO<sub>x</sub> is further prescribed as a function of NO<sub>x</sub> concentration. **We have now modified Eq. 2 and the relevant text:**

195 By leveraging WRF-Chem's chemical diagnostic ~~feature capability~~ feature capability, we derive the net chemical tendency of NO<sub>x</sub> within each hour [R<sub>NO<sub>x</sub></sub>, ppb hr<sup>-1</sup>] ~~per model grid for every model grid within the lower 12 vertical levels~~ (x, y)-based on the output cumulative chemical ~~(x, z). R<sub>NO<sub>x</sub></sub> is calculated specifically from the cumulative~~ changes in NO and NO<sub>2</sub> concentrations solely due to chemical reactions (i.e., "chem\_no2" and "chem\_no" in WRF-Chem registry) following **Eqs. 2:**

$$\sum_{h_0}^h \Delta C_{NO_x}(x, y, z) = \sum_{h_0}^h \Delta C_{NO}(x, y, z) + \sum_{h_0}^h \Delta C_{NO_2}(x, y, z) \quad (2a)$$

200 
$$R_{NO_x}(x, y, z, h) = P_{NO_x}(x, y, z, h) - L_{NO_x}(x, y, z, h) = \frac{\sum_{h_0}^h \Delta C_{NO_x}(x, y, z) - \sum_{h_0}^{h-1} \Delta C_{NO_x}(x, y, z)}{1 \text{ hr}} \quad (2b)$$

where model hour h denotes the ~~beginning time of the hour interval of the hourly WRF-Chem outputs~~ start time of each hour interval in the WRF-Chem outputs and z denotes ~~the index of model vertical levels~~ (i.e., from 1 to 12).  $\sum_{h_0}^h \Delta C_{NO_x}$  describes the cumulative net changes to NO<sub>x</sub> concentration given chemical reactions from the initial model hour h<sub>0</sub>.



5. It would be useful to assess the consistency of the NO<sub>x</sub> chemical lifetime from WRF-Chem to the available observations, although limited.

We agree that assessing WRF-Chem against observations would be useful. However, the main goal of this study is not to determine if the RACM2 chemical scheme in WRF-Chem is correct, but to investigate if a simplified model can replace a sophisticated chemical scheme, assuming it is correct. There had been numerous studies aiming to evaluate and improve WRF-Chem chemical schemes. Lastly, we recognize that our simplified NO<sub>x</sub> curves can be improved and replaced.

NO<sub>2</sub>-to-NO<sub>x</sub> ratio (Sect. 2.2):

1. The reactions of NO + HO<sub>2</sub> and NO + RO<sub>2</sub> to form NO<sub>2</sub> are excluded, but they are important in the boundary layer.

We agree that RO<sub>2</sub>/HO<sub>2</sub> are additional sources to oxidize NO, which is missing from the estimate of the NO<sub>2</sub>-to-NO<sub>x</sub> ratio (that relies on modeled NO<sub>x</sub> values and a prescribed O<sub>x</sub> level of 50 ppb, which neglects local O<sub>x</sub> variability with VOC reactivity as discussed in **Sect. 5.3.1**). Properly resolving such reactions requires knowledge/input of VOC emission and chemistry, which would be even more challenging and essentially requires a full chemistry model. Yet, there may be room for simple parameterizations as further discussed in **Sect. 5.3.1**, including 1) adding background ozone, tracking ozone or its production rate along trajectories by leveraging satellite column observations of HCHO, and 2) parameterizing the NO<sub>2</sub>-to-NO<sub>x</sub> ratio as a function of feature variables including VOC<sub>R</sub>. **Relevant modifications to Sect. 5.3.1 are attached as follows:**

VOC<sub>R</sub> may also affect the O<sub>x</sub> level, ~~thus, the and the~~ NO<sub>2</sub>-to-NO<sub>x</sub> ratio. The prescribed O<sub>x</sub> level of 50 ppb neglected the (Sect. 2.2) overlooks the nonlinear O<sub>x</sub> variability given its similar non-linear dependence on concentrations and related to VOC<sub>R</sub> (Murphy et al., 2007; Li et al., 2022). Specifically, In NO<sub>x</sub>-limited scenarios, OH favors the oxidation of VOCs, and local-scale O<sub>x</sub> is primarily predominately produced by NO + RO<sub>2</sub> or NO + HO<sub>2</sub> under limited rich conditions. Consequently, higher, suggesting higher O<sub>x</sub> levels with increased NO<sub>x</sub> concentrations result in higher levels. However, The omission of NO + RO<sub>2</sub> or HO<sub>2</sub> in Eqs. 3 could lead to an underestimation of the NO<sub>2</sub>-to-NO<sub>x</sub> ratio, which likely explains the modeled tNO<sub>2</sub> being consistently lower than observations over background regions. Conversely, under NO<sub>x</sub>-saturated conditions, the production-of-consumption of OH by NO<sub>x</sub> may limit the VOC oxidation and O<sub>x</sub> is suppressed-by-production, leading to a decline in O<sub>x</sub> level as NO<sub>x</sub> concentration increases. For example, rises. Consequently, the NO<sub>2</sub>-to-NO<sub>x</sub> ratio might be overestimated when true O<sub>x</sub> levels may be lower than fall below 50 ppb at saturated regimes. If a simplified (particularly under stagnant atmospheric mixing) or underestimated due to the absence of NO + RO<sub>2</sub> reactions. Nevertheless, our pre-determined O<sub>x</sub> nonlinearity is implemented, the conversion from NO to would be further slowed to alleviate strong overestimation of tropospheric under stagnant mixing conditions. Nonetheless, our prescribed level of 50 ppb serves acts as a first-order eap to prevent the endless non-physical conversion limit to prevent unrealistic conversion from NO to from NO when NO<sub>2</sub> at extremely high NO<sub>x</sub> is extremely high since levels when O<sub>3</sub> can be is being titrated.

To address these limitations, one potential approach is to leverage formaldehyde concentrations retrieved from TROPOMI. Recent studies revisited the use of the formaldehyde-to-NO<sub>2</sub> ratios (i.e., FNR) from satellites as a means of inferring O<sub>3</sub> production rates (Goldberg et al., 2022; Sourì et al., 2022). Our WRF-Chem simulations, which were used to parameterize the NO<sub>x</sub> chemical tendency, show that modeled formaldehyde generally increases with VOC<sub>R</sub> with varying slopes influenced by SZA and NO<sub>x</sub> concentrations (**Supplement Fig. S18c**); and O<sub>3</sub> concentrations scale non-linearly with FNRs with O<sub>3</sub> concentration approaching a background value at high FNR > 10 (**Supplement Fig. S18d**). Even though satellite-based FNRs may theoretically help probe O<sub>3</sub> or O<sub>x</sub> concentration to better parameterize NO<sub>2</sub>-to-NO<sub>x</sub> ratios, Sourì et al. (2022) stressed that retrieval errors especially from formaldehyde (40 to 90% with ≤ 50% over cities) and inherent chemical errors of the predictive power of FNRs may hinder the broad application of space-based FNRs at the current stage. Nonetheless, sensitivity analyses in **Sect. 3** indicate an overall chemical uncertainty in tNO<sub>2</sub> of about 10 to 20% with respect to NO<sub>2</sub> signals, even if perturbed O<sub>x</sub> level is much lower than 50 ppb (**Fig. 4**).

2. Line 242: Please clarify how the NO<sub>x</sub> chemical tendency in the model change when ozone is titrated near high emitters.

We clarify that in STILT-NO<sub>x</sub>, only NO<sub>x</sub> (no ozone) is tracked and updated per timestamp along the trajectory; and the calculation of NO<sub>x</sub> chemical tendency relies on NO<sub>x</sub> concentrations and SZA. Thus, RNO<sub>x</sub> would not change as ozone decreases in the model. See our sensitive analysis above about the performance of estimating RNO<sub>x</sub> using additional variables (see our earlier response to the second comment).

The initial text was to explain how the NO<sub>2</sub>-to-NO<sub>x</sub> ratio parameterized separately from RNO<sub>x</sub> would decrease when NO<sub>x</sub> emission/concentrations become extremely high (titrating ozone). Such titrations near high NO<sub>x</sub> emitters are controlled by the prescribed total oxidant level, [Ox] = [O<sub>3</sub>] + [NO<sub>2</sub>], despite a simple constant value being assigned (see response above for limitation of this constant Ox level). For example, if a STILT-NO<sub>x</sub> air parcel passes by a larger emitter like a power plant, its tagged NO<sub>x</sub> concentration will be largely enhanced but its final NO<sub>2</sub> column at the receptor/sounding location may stay low given limited oxidant capacity.

Eq 1: The processes of NO<sub>2</sub> dry deposition and mixing between the mixed layer and the free troposphere seem to be neglected.

We thank the reviewer for pointing out those physical processes. We agree that neglecting the dry deposition of NO<sub>2</sub> or NO may overestimate their concentrations and alter the estimated chemical tendency of NO<sub>x</sub> along the trajectories that further feedback to the concentrations. Previous studies implemented the deposition module that relies on the key estimation of “dry deposition velocity” for air parcels residing within the lower 50 m from the surface layer (e.g., Wen et al., 2011). Moreover, the mixing between the mixed layer and the free troposphere (FT) was neglected and requires future model modifications, such as 1) quantification of the entrainment zone and 2) the choice of vertical mixing time-/length- scales at the PBL-FT interface. Although issues with mixing and deposition were not fully resolved in this study, **we acknowledge these limitations and discuss possible future improvements in Sect. 5.3.2:**

### **5.3.2 The impact from emission profiles and inter-parcel mixing scales**Uncertainties in non-chemical processes

Besides simplification of chemical reactions, modeled tNO<sub>2</sub> values can be subject to a few physical processes and parameters, including emission profiles, inter-parcel mixing scales, and dry deposition.

The underlying STILTv2 (Fasoli et al., 2018) accounted for a gradual growth of the mixed layer height over the hyper-near-field area around emissions. ~~Convolving. Yet, by convolving~~ the STILT footprint with NO<sub>x</sub> emissions, we assumed that emissions ~~originating-originate~~ from the surface ~~and~~ are uniformly mixed over the mixed layer without considering the possible uneven distribution of emissions from different vertical levels. In reality, under stable atmospheric conditions, the stack heights or plume heights of emission sources can sometimes extend above the shallow PBL. Our current assumption may thus lead to an overestimation in modeled concentrations, and such biases can in turn affect the estimate of NO<sub>x</sub> tendency. More importantly, changes in the vertical ~~emission-profile-profile of emissions~~ can lead to changes in concentration per model level, which ~~also~~ affect the tropospheric ~~column-results-columns~~ as the typical averaging kernel profile is far from uniform within the PBL. Recall that TROPOMI NO<sub>2</sub> AKs decreases rapidly towards the surface (**Fig. 1**). Hence, placing ~~a-an emission~~ plume at the surface or ~~at~~ an elevated altitude (e.g., 400 m) can cause a discrepancy in ~~the-modeled-column-values-modeled column concentrations. In~~

670 addition, if the wind shear is strong over an intensive point source (likely the Intermountain example in Fig. 5c), assumptions in the injection height and vertical profile of emission plumes may affect the modeled plume shape and possibly deviate the estimated near-field wind bias following Sect. 5.2.1. Noticeably, Maier et al. (2022) ~~implemented~~ investigated the influence of inaccurate representation of emission profiles on the flask-like modeled concentrations by implementing a time-varying sector-specific emission profile into STILT. ~~Yet, the influence~~ ~~Such an impact~~ on column concentrations ~~due to changes in emission profiles may require more~~ ~~may be minimized but yet requires future~~ in-depth investigations, particularly over point sources.

Accounting for inter-parcel mixing was an important aspect when developing Lagrangian chemical models. Omitting inter-parcel mixing makes solving for non-linear processes (such as chemical NO<sub>x</sub> loss) problematic. On the contrary, Eulerian models suffer from excessive numerical diffusion. Mixing that is too strong smooths the spatial gradient of concentration and can lower the concentration within the fixed model grids, which may cause slight shifts in NO<sub>x</sub> regimes. Valin et al. (2011) 675 suggested that a spatial resolution of 4 to 12 km is sufficient to capture the non-linearity in NO<sub>x</sub> loss rate. As for Lagrangian models, efforts can be made to enable the flux exchange between air parcels via deformations (Konopka et al., 2019; McKenna et al., 2002). ~~STILT realized the~~ ~~In addition to the inter-pacel mixing within the mixed layer (ML), several other turbulent mixing processes require future investigation, including (1) horizontal mixing in the free troposphere (FT), (2) vertical mixing~~ 680 ~~between the ML and FT, and (3) mixing between tracked air parcels with the untracked surrounding background. For example, Real et al. (2008) utilized a linear relaxation with exponential decay of the plume concentrations towards the background based on a timescale of 2 days to address the third mixing process. The second mixing process requires future modifications involving the determination of entrainment zones and mixing hyperparameters for such ML-FT exchange.~~

~~The original STILT model realized~~ vertical mixing by diluting surface emissions ~~over~~ ~~across~~ the ML height (Lin et al., 2003). ~~We and we~~ further enabled an exchange in pollutants' concentrations with prescribed mixing length- and ~~time~~-scales 685 ~~following (Wen et al., 2012). As a final sensitivity test~~ ~~time-scales representing typical horizontal mixing rates (Sect. 2.3). As final sensitivity tests,~~ we simulated tNO<sub>2</sub> ~~using~~ ~~based on~~ a spectrum of mixing hyperparameters ~~over~~ ~~for~~ the New Madrid power plant ~~and found minimal influence on modeled values per sounding (uncertainty < 20%,~~ ~~Uncertainties in the mixing parameters result in minimal uncertainties on the sounding-level modeled tNO<sub>2</sub> values (Supplement Fig. S19). For example,~~ 690 ~~differences in modeled tNO<sub>2</sub> between the mixing and non-mixing simulations become larger as mixing becomes faster and for receptors/soundings located on the edge of the plume (i.e., only a small fraction of the trajectories encountered power plant emission in Supplement Fig. S20).~~ Uncertainties in the prescribed mixing hyperparameters contribute even less to the modeled values over urban areas (i.e., < 10% for Phoenix cases), where emissions are generally better mixed than at power plants. ~~In addition, such mixing influence can vary with the spatial resolution of the emission inventory used in the simulations.~~

695 ~~The dry deposition of NO<sub>2</sub> was not factored into this study, which could lead to an overestimation of modeled NO<sub>2</sub>. For future model implementations, it is possible to track loss of NO<sub>2</sub> concentrations due to dry deposition by calculating "dry deposition velocities" (e.g., ?) when air parcels descend close to the surface, e.g., 50 meters above the surface (Wen et al., 2012).~~

Eq. 5 assumes that the model transport and chemistry errors are independent, when in fact these errors are related.

While it is difficult to fully separate the transport error from the chemistry error (since the physical and chemical processes are fully coupled), our transport error analysis that involves perturbing wind fields and recalculating [NO<sub>x</sub>] along trajectories implicitly contains errors in tNO<sub>2</sub> due to errors in wind and chemistry. This can be explained as follows:

Imagine a modeled air parcel/trajectory passing over a point source in the default run. With a small perturbation to the model winds, the air parcel no longer passes over that point source. The NO<sub>x</sub> concentration of these two air parcels would be different for two reasons:



- 1) the wind fields are perturbed → leading to changes in emissions and NO<sub>x</sub> concentrations (e.g., lower values for the perturbation run); and
- 2) the associated feedback involving chemistry → lower NO<sub>x</sub> concentration in the end simulation leads to changes in chemical tendency (and so on for further timesteps).

Our linear combination of three error sources would likely have been a conservative estimate given the nature of the transport error analysis. An alternative approach is to perturb the wind fields and the chemistry simultaneously to account for the covariance between the two sources of uncertainties, which is hard to realize with existing tools.

Fig. 5 and elsewhere: Please clarify how tNO<sub>2</sub>, the tropospheric NO<sub>2</sub> column, is converted to a volume mixing ratio.

Thanks for this comment. We clarify that “tNO<sub>2</sub>” denotes the tropospheric NO<sub>2</sub> mixing ratio that is derived from the initial tropospheric NO<sub>2</sub> vertical column density (VCD). **We now add a brief explanation to the introduction section when tNO<sub>2</sub> is first brought up:**

In this study, we present a non-linear modeling framework, STILT-NO<sub>x</sub>, to simulate tropospheric **column-average** NO<sub>2</sub> **columns mixing ratio** (tNO<sub>2</sub>) as retrieved from TROPOMI. **Note that initial NO<sub>2</sub> vertical column density [VCD, molec cm<sup>-2</sup>] is converted to tNO<sub>2</sub> [ppb] by dividing by a dry air VCD. The dry air VCD is calculated by integrating a profile of the ideal gas number density of air minus a modeled water vapor profile.**

Line 382: Considering the model’s sensitivity to errors in the wind direction and speed, it may be better to use winds from reanalyses datasets or to bias correct the model using nearby observations. This seems important for the inversion work planned in the future. Are there other ways to reduce this error?

Yes – as emphasized in Sect. 5, wind biases affect the interpretation of the model-data alignment of column NO<sub>2</sub> and other species and possibly the corresponding inverted fluxes/emissions. We note that meteorological reanalyses with relatively coarse spatiotemporal resolutions are not real observations and are associated with uncertainties. For example, the GFS meteorological field driving STILT is a data assimilation (reanalysis) product but still cannot resolve highly fine-scale wind patterns. Moreover, the nearby observations are spatially limited, e.g., the radiosonde observations used for regional wind assessment and transport error estimates (Sect. 3).

We may further differentiate random wind errors from systematic wind biases. The former error can be quantified (Sect. 3) and usually be propagated into the observational error matrix during the inversion. It is the wind biases that have hardly been addressed in inversion studies. Possible approaches as we discussed in Sect. 5.2.1 include the rotation of plumes or a more sophisticated data assimilation approach to correct emissions and wind altogether (e.g., Liu et al., 2017). In the ongoing inversion work, we will design and conduct OSSE to investigate the quantitative impact of wind biases on inverted fluxes and explore ways to explicitly address the wind error.

Lines 564-570: These lines are unclear.

As shown in Fig. 1, the two essential competing loss pathways of NO<sub>x</sub> are NO<sub>2</sub> + HO → HNO<sub>3</sub> and NO + RO<sub>2</sub> → RONO<sub>2</sub> with a minor branching ratio (typical value of 0.04 and further depends on

the R groups). In other words, when VOC<sub>R</sub> stays high and NO<sub>x</sub> is limited, there is a tendency to form RONO<sub>2</sub> over HNO<sub>3</sub>, which explains why the trough of the NO<sub>x</sub> curves shifts to the higher end of NO<sub>x</sub> concentration as shown in Fig. 10. We have reworded these lines as follows:

When considering lower SZAs (consistent with TROPOMI overpass time of 1 pm TROPOMI observations local time), the general non-linear shape characteristic of these NO<sub>x</sub> curves holds as VOC<sub>R</sub> increases (Fig. 10). Higher VOC<sub>R</sub> relative to the lower NO<sub>x</sub> concentration favors the oxidation of VOCs and the by OH and the associated minor loss pathway of NO + RO<sub>2</sub> to form alkyl nitrates with a small branching ratio over the minor branching ratio, over the competing major NO<sub>x</sub> loss pathway of NO<sub>2</sub> + OH (Fig. 1). To compete with the VOC oxidation in reacting with OH with rising VOC<sub>R</sub>, the NO<sub>x</sub> loss tendency becomes slower (chemical tendency becomes more positive (P - L, Supplement Fig. S18a) and concentrations at the optimal point (where two loss pathways reach their maximums) must be increased, as illustrated by the increasing from 1.4 to 3.7 ppb the net loss timescale elongates (e.g., ts<sub>min</sub> from 2 to 4 hours in Fig. 10. For the same reason, the net loss timescale (ts<sub>NO<sub>x</sub></sub>) generally rises as increases,). Moreover, NO<sub>x</sub> is required to reach a higher level to compete with the reactions involving VOCs, evident by the shift in the trough of the NO<sub>x</sub> curves (e.g., from about 2 to 4 hours NO<sub>x</sub> min from 1.4 to 3.7 ppb in Fig. 10). To put it in context, the NO<sub>x</sub> curves shown in Fig. 3 represent the typically curves under moderate typical patterns as long as VOC<sub>R</sub> (e.g., < remains below 10 s<sup>-1</sup>). Elevations in ts<sub>NO<sub>x</sub></sub> with may be problematic when NO is high because the ts<sub>NO<sub>x</sub></sub> has already been quite high; while more erroneous under conditions with moderate NO and extremely high of over 10 s<sup>-1</sup>.

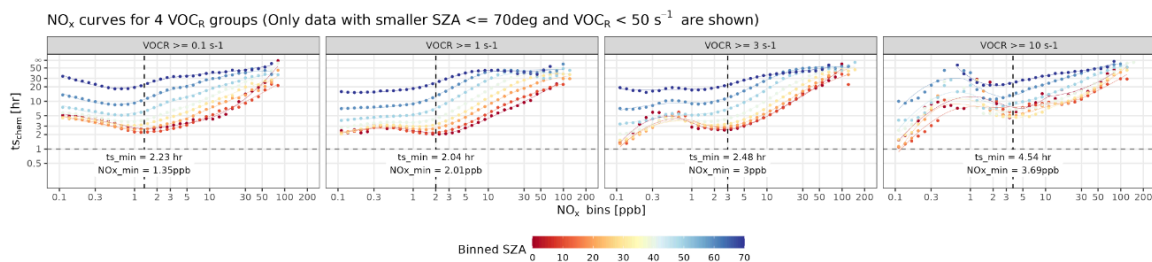


**Figure 10.** (a) Similar to Fig. 3b, but differentiated by 4 intervals of VOC<sub>R</sub> and SZA bins smaller than 70 degrees with an a spacing of 10 degrees. All panels here utilized model results from the same WRF-Chem simulations described in Sect. 2 and Appendix A.